Fringing fields in disc capacitors

1986 J. Phys. A: Math. Gen. 19 2725

(http://iopscience.iop.org/0305-4470/19/14/012)

J. Phys. A: Math. Gen. 19 (1986) 2725-2736. Printed in Great Britain

Fringing fields in disc capacitors

G J Sloggett†, N G Barton‡ and S J Spencer†

† CSIRO Division of Applied Physics, Sydney, Australia 2070

‡ CSIRO Division of Mathematics and Statistics, Sydney, Australia 2070

Received 2 October 1985

Abstract. The results of a high accuracy numerical study of the uniformity of the electric field between parallel disc electrodes are reported. Simple analytical expressions are derived describing the field behaviour at points on the electrodes near the edges of the discs and also at points between the electrodes remote from the edges. These expressions are consistent with the numerical results. A simple approximation for the fringing capacitance of parallel-plate electrode systems of arbitrary shape is also given. This expression leads to a first-order approximation for the total capacitance which, for disc electrodes, has superior accuracy to similar published approximations for radii up to five times the disc separation. A higher-order approximation for the capacitance is shown to have markedly better accuracy than any first-order approximation.

1. Introduction

In electrostatic problems involving unguarded parallel-plate electrodes, the interelectrode electric field departs from uniformity, especially near the plate edges, and extends into space beyond the electrodes. These departures from ideal uniform field behaviour are often referred to as 'fringing', and for certain applications are highly significant. For example, the elementary expression for the capacitance of parallel-plate capacitors ($C_{\text{elem}} = \varepsilon A/d$ with ε the dielectric constant, A the plate area and d the plate separation) underestimates the true capacitance because it ignores the fringing field. Fringing effects are also important in systems designed to achieve highly uniform fields. An example is an electrometer constructed as an absolute standard of voltage, in which it is necessary to achieve a field non-uniformity not exceeding one part in 10^7 (Sloggett *et al* 1984). This instrument has essentially a disc and plane electrode geometry as shown in figure 1, and is equivalent, by the principle of images, to two coaxial discs. The region in which high field uniformity is required lies within a small radius of the axis of symmetry.

In the last hundred years, a number of authors have given calculations for the potential distribution between disc electrodes at equal or opposite potential. The most comprehensive work is due to Nicholson (1924) and Love (1949) who used an expansion for the potential in terms of oblate spheroidal coordinates. The boundary condition on the discs gives rise to a Fredholm integral equation of the second kind which was solved iteratively by Bartlett and Corle (1985). Bartlett and Corle confirmed their solution by a separate numerical procedure based upon finite differences. In other work, Atkinson *et al* (1983) claimed to have solved the potential problem by a Hankel transform technique, although Hughes (1984) pointed out that their method was in error as it did not give a continuously differentiable solution.

0305-4470/86/142725+12$02.50

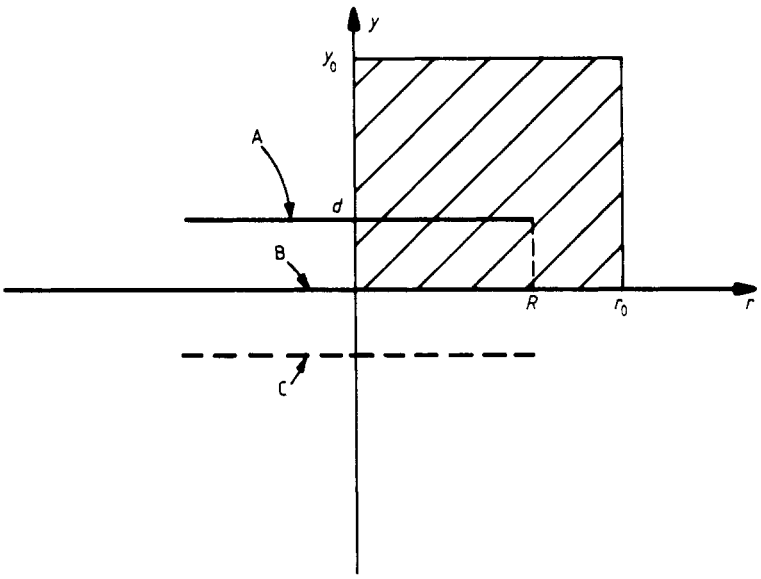

Figure 1. Geometry of disc and plane electrode system. A, disc electrode ($\phi = V$); B, plane electrode ($\phi = 0$); C, image electrode ($\phi = -V$).

The published literature provides little quantitative information on the field uniformity. For this purpose, an evaluation of the potential distribution to a very much higher accuracy than that obtained by Bartlett and Corle is required. Such an evaluation has been carried out by Harrison (1967) for various electrode profiles designed for electrical discharge studies. In this paper, we present the results of a numerical investigation of field uniformity for the flat electrode geometry of figure 1. We also provide analytical confirmation of some key numerical results, and study analytically the behaviour of the capacitance due to fringing fields.

2. Numerical investigation of the disc–plane potential problem

The axisymmetric electric potential ϕ satisfies Laplace's equation

$$\frac{\partial^2\phi}{\partial r^2}+\frac{1}{r}\frac{\partial\phi}{\partial r}+\frac{\partial^2\phi}{\partial y^2}=0 \tag{1}$$

in which (r, ϕ, y) are the usual cylindrical polar coordinates. Standard algorithms (see, for example, DiStasio and McHarris 1979) based on Jacobi iteration were used to evaluate ϕ at a grid of points $(i\Delta r, j\Delta y)$, where Δr and Δy are grid increments in the radial and vertical directions respectively. For the geometry of figure 1, we solved for $y \geq 0$ and $r \geq 0$ with the boundary conditions

$$\phi = V \qquad \text{for } y = d \text{ and } r \leq R \tag{2}$$

$$\phi = 0 \qquad \text{for } y = 0 \tag{3}$$

and

$$\frac{\partial\phi}{\partial r}=0 \qquad \text{for } r = 0. \tag{4}$$

The last condition results from axial symmetry. For computational purposes, we introduced outer boundaries $r = r_0$ and $y = y_0$ as shown in figure 1, and set $\phi = 0$ on both boundaries.

The radial and vertical components of the electric field, denoted E_r and E_y respectively, were calculated directly from the array of potentials. These are most usefully expressed in normalised form:

$$\varepsilon_r = E_r d / V \tag{5}$$

and

$$\varepsilon_y = E_y d / V. \tag{6}$$

The non-uniformity of the field in the interelectrode region has two components, namely the radial, which is just ε_r, and the vertical, δ_y, which is given by

$$\delta_y = \varepsilon_y - 1. \tag{7}$$

The principal computational goal was to evaluate field non-uniformities as small as 10^{-8} to an accuracy of 3% or better. Thus double precision accuracy was required in computing the potentials. Parameters r_0, y_0, Δr and Δy were chosen to minimise the size of the potential array consistent with the accuracy goal. Preliminary trials established the following values for a given electrode radius R and separation d:

$$\begin{aligned} r_0 &= R + 10d \\ y_0 &= 5d \\ \Delta r &= d/10 \\ \Delta y &= d/20. \end{aligned} \tag{8}$$

As an example, for $R/d = 10$ the array size was 201×101 points.

Preliminary convergence tests using over-relaxation were found to give oscillatory non-convergent behaviour. This may be a consequence of the zero thickness of the disc electrode. DiStasio and McHarris (1979) suggest that a requirement for accelerated convergence is that the grid increments be smaller than the smallest linear dimension of the electrode geometry, a condition not met in the present case. Thus an acceleration factor of unity was used, and convergence was found to be slow. Ultimately, 2200 iterations were performed for each run and comparisons were made with the result after 2000 iterations to confirm accuracy. This number of iterations was sufficient to evaluate field non-uniformities as small as 10^{-12}, and the required accuracy was achieved at all points other than within one or two grid increments of the edge of the disc.

Potentials and fields were computed for values of R/d from 2 to 20. Representative results, for $R/d = 8$, are shown in the form of interpolated contour maps in figure 2. The equipotentials (figure 2(a)) show the influence of fringing at the edge of the upper electrode and are comparable with the results of Bartlett and Corle (1985).

Contours of equal vertical field non-uniformity, δ_y, are shown in figure 2(b). It may be seen that, at points more than one or two multiples of d in from the edge of the disc, the field non-uniformity penetrates in a regular and exponentially decreasing manner into the gap. For a given radius, extrema of field non-uniformity occur on the electrodes, with maxima (i.e. points of maximum field magnitude) on the disc electrode and minima on the plane electrode. The normalised radial field (figure 2(c)) also shows exponential decay with penetration into the gap, but exhibits a maximum for a given radius at a point midway between the electrodes. The radial field is directed outwards for $V > 0$.

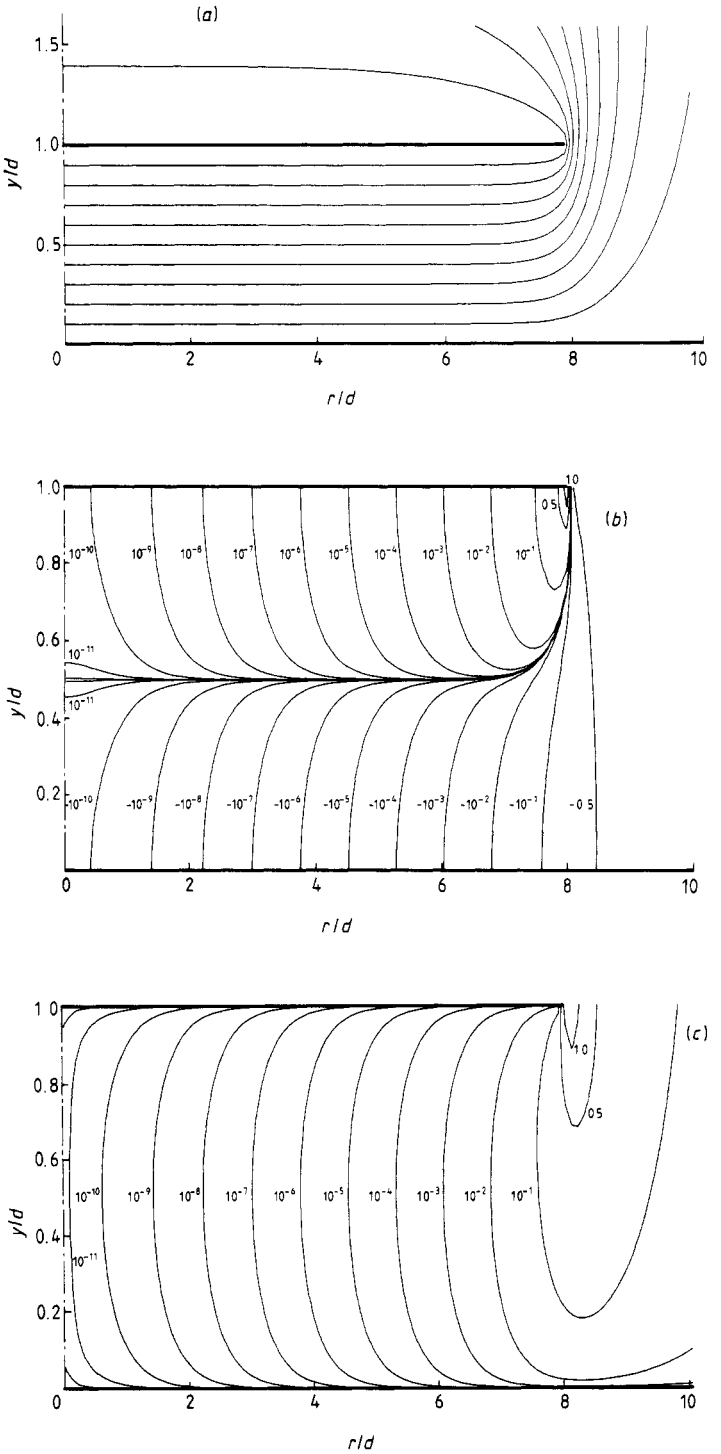

Figure 2. Contour plots of numerical results for disc and plane electrodes, $R/d = 8$: (*a*) equipotentials at 0.1 V increments, (*b*) non-uniformity of vertical field δ_y and (*c*) normalised radial field ε_r.

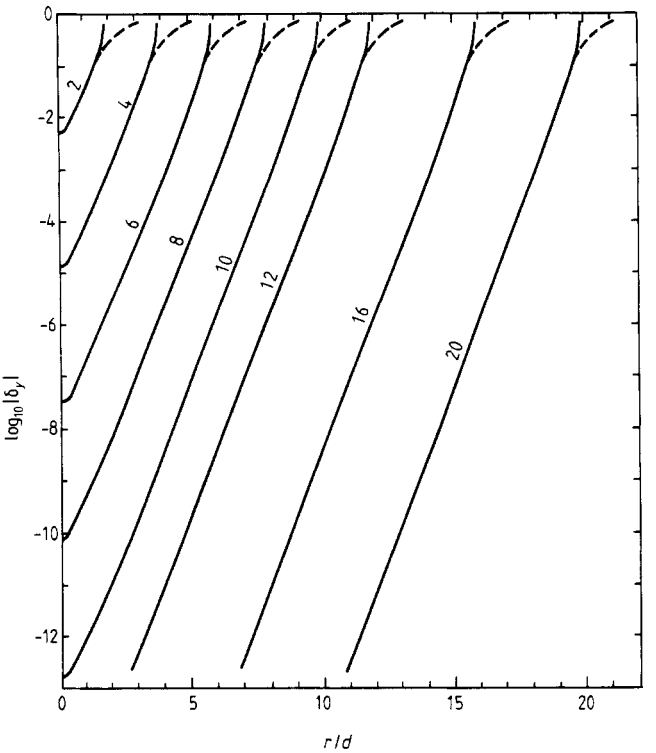

Figure 3. Computed vertical field non-uniformity δ_y on disc and plane electrodes for R/d values of 2-20. δ_y has positive sign on the disc (full curve), and negative sign on the plane (broken curve).

Figure 3 shows the behaviour of $|\delta_y|$ on both electrodes for a range of values of R/d. The region of exponential decay is seen to correspond, approximately, to $d < r < R - d$, and the rate of decay is 1.34 decades per unit reduction in r/d for $R/d = 20$. The vertical field non-uniformity has a singularity at the edge of the disc electrode, and tends to -1 (since $E_y \to 0$) as $r \to \infty$ on the plane electrode. At $r = 0$ on either electrode the field non-uniformity attains a minimum value given by the empirical law

$$|\delta_y| = 2.57 \times 10^{-1.32R/d}. \tag{9}$$

Figure 3 permits the straightforward assessment of maximum field non-uniformity in any problem having the geometry of figure 1. In the case of the absolute volt apparatus, for example, the minimum value of R/d is 9.7. Over the critical central region, corresponding to $r/d < 1.1$, we find that $|\delta_y| < 2 \times 10^{-12}$, several orders of magnitude below the experimental requirement.

3. Theoretical analysis

In this section, we derive theoretical results for the potential near the edge of the disc electrode for the case when R/d is large. The results are based on the approximation of the edge of the disc electrode by a semi-infinite straight-edged plane. The potential problem in this geometry becomes two-dimensional (see figure 4(a)) and, as first shown

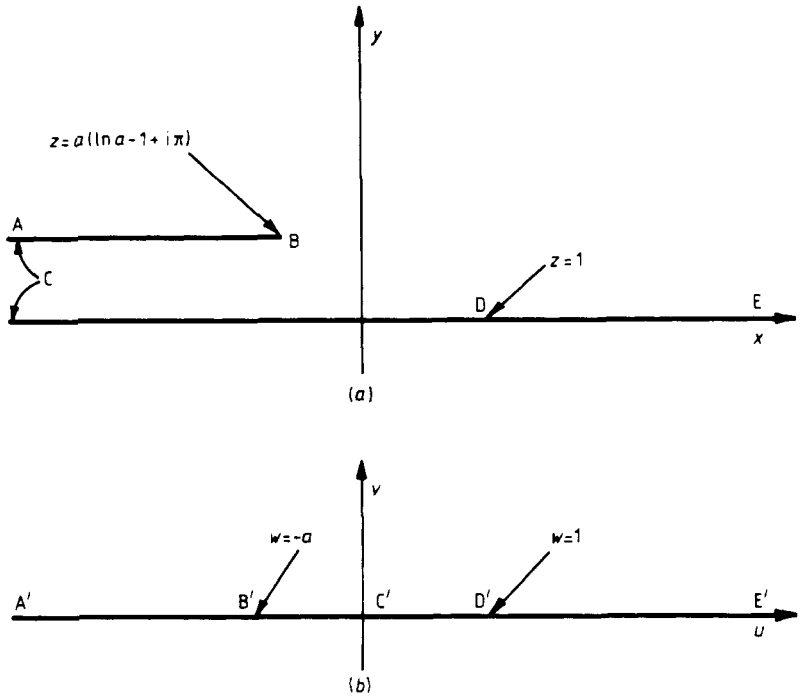

Figure 4. Two-dimensional electrode geometry in (a) the z plane, $z = x + iy$, and (b) the w plane, $w = u + iv$.

by Maxwell (1904), may be treated by conformal mapping methods. From Kober (1957), the upper half of the complex z plane ($z = x + iy$) in figure 4(a) is mapped to the upper half of the complex w plane ($w = u + iv$) by the Schwarz-Christoffel conformal map

$$z = w + a \ln w \tag{10}$$

where $a = d/\pi$. The electrode system ABCDE in the z plane maps to the points A'B'C'D'E' on the real axis of the w plane (figure 4(b)). In the w plane, the upper half-plane problem is to solve Laplace's equation subject to the boundary conditions

$$\phi(u, 0) = \begin{cases} V & u < 0 \\ 0 & u > 0 \end{cases} \tag{11}$$

and, by standard arguments (see, e.g., Carrier *et al* 1966), the solution is

$$\phi(u, v) = \frac{1}{\pi} \int_{-\infty}^{\infty} \frac{\phi(s, 0)}{(u - s)^2 + v^2} \, ds$$

or

$$\phi(u, v) = \frac{V}{\pi} \tan^{-1} \frac{v}{u} = \frac{V}{\pi} \operatorname{Im}(\ln w). \tag{12}$$

Now the electric field components are given by evaluating $\partial\phi/\partial x$ and $\partial\phi/\partial y$ as follows. Define $G = (V/\pi) \ln w$; then

$$\frac{\partial \phi}{\partial x} = \operatorname{Im}\left(\frac{\partial G}{\partial x}\right) = \operatorname{Im}\left(\frac{dG}{dz}\right) = \operatorname{Im}\left(\frac{dG}{dw}\left(\frac{dz}{dw}\right)^{-1}\right)$$

$$\frac{\partial\phi}{\partial y}=\mathrm{Im}\left(\frac{\partial G}{\partial y}\right)=\mathrm{Im}\left(\mathrm{i}\frac{\mathrm{d}G}{\mathrm{d}z}\right)=\mathrm{Re}\left(\frac{\mathrm{d}G}{\mathrm{d}z}\right)=\mathrm{Re}\left(\frac{\mathrm{d}G}{\mathrm{d}w}\left(\frac{\mathrm{d}z}{\mathrm{d}w}\right)^{-1}\right).$$

Since $\mathrm{d}z/\mathrm{d}w=(w+a)/w$, we have that

$$E_x=\frac{\partial\phi}{\partial x}=\frac{V}{\pi}\mathrm{Im}\left(\frac{1}{w+a}\right) \tag{13a}$$

$$E_y=\frac{\partial\phi}{\partial y}=\frac{V}{\pi}\mathrm{Re}\left(\frac{1}{w+a}\right). \tag{13b}$$

In the case of points on the electrodes we have $v=0$, from which it follows that E_x vanishes, as expected, and

$$E_y=\frac{V}{\pi(u+a)}. \tag{14}$$

We now interpret these results in our original (x, y) coordinate system. For points on the underside of the upper electrode and near to its edge B, we may write

$$z=a(\ln a-1-\mathrm{i}\pi)-t \tag{15a}$$

and

$$w=u=-a+s \tag{15b}$$

where s and t are real and positive and t measures distance from the edge of the electrode. Substituting in equation (10) and expanding the ln term, we find that, for small s and t,

$$s=(2at)^{1/2} \tag{16}$$

and, from equation (14),

$$E_y=\frac{V}{\pi}(2at)^{-1/2}=V(2\pi dt)^{-1/2}. \tag{17}$$

This equation describes the singular behaviour of E_y near the edge of a disc of large radius.

Points which are between the electrodes and remote from the edge correspond to w near 0 in figure 4(b). For $|w|$ sufficiently small, equation (10) gives

$$w\approx\mathrm{e}^{z/a}=\mathrm{e}^{x/a}\left(\cos\frac{y}{a}+i\sin\frac{y}{a}\right) \tag{18}$$

and equations (13a) and (13b) therefore give

$$E_x\approx\frac{V}{\pi a}\mathrm{Im}\left(1-\frac{w}{a}\right)\approx-\frac{V}{\pi a^2}\mathrm{e}^{x/a}\sin\frac{y}{a} \tag{19a}$$

$$E_y\approx\frac{V}{\pi a}\mathrm{Re}\left(1-\frac{w}{a}\right)\approx\frac{V}{\pi a}\left(1-\frac{1}{a}\mathrm{e}^{x/a}\cos\frac{y}{a}\right). \tag{19b}$$

Finally, making the substitutions $a=d/\pi$ and $x=a(\ln a-1)-t$, where t is again the distance from the edge of the upper electrode, it follows that the field non-uniformities are

$$\delta_x\approx-\exp[-(1+\pi t/d)]\sin\pi y/d \tag{20a}$$

$$\delta_y\approx-\exp[-(1+\pi t/d)]\cos\pi y/d. \tag{20b}$$

These equations describe the behaviour seen in figures 2(*b*) and 2(*c*) for points between the electrodes and not too near the edge of the disc. At points on the electrodes $|\delta_y|$ takes its maximum value for a given value of t,

$$|\delta_y| = \exp[-(1+\pi t/d)] = \frac{1}{e}10^{-1.364\,t/d}. \tag{21}$$

$|\delta_x|$ takes the same maximum value, but at $y = d/2$.

Some representative data calculated from equation (21) are given in table 1, together with corresponding numerical data for disc electrodes of two different radii. It may be seen that, at a given distance from the edge of the disc, $|\delta_y|$ increases slowly as disc radius decreases. This seems physically reasonable since a reduction in the disc radius will tend to bring the edge nearer, on average, to any point at a fixed radial distance t from it. The table shows that, as an approximation to the behaviour of field non-uniformity on disc electrodes, equation (21) is best for large values of R/d and small values of t/d. The rate of decrease of field non-uniformity with increasing t given by equation (21) (1.364 decades per multiple of d) slightly underestimates the rate for disc electrodes. Examination of the numerical results shows that, in this respect also, equation (21) is a better model for discs of large radius than for discs of small radius.

Table 1. Values of $|\delta_y|$ on disc electrodes of various radii. Data for $R/d = 10$ and $R/d = 20$ are obtained numerically; data for $R/d = \infty$ from equation (21).

t/d	$R/d = 10$	$R/d = 20$	$R/d = \infty$
2	8.58×10^{-4}	7.88×10^{-4}	6.87×10^{-4}
4	1.92×10^{-6}	1.62×10^{-6}	1.28×10^{-6}
6	4.61×10^{-9}	3.38×10^{-9}	2.40×10^{-9}
8	1.30×10^{-11}	7.20×10^{-12}	4.47×10^{-12}

4. Capacitance

We may use the above analysis to study the fringing capacitance and hence the total capacitance of parallel-plate electrodes. Fringing capacitance is defined as the additional capacitance beyond that which would be expected if the field were uniform and equal to V/d between the electrodes, and zero elsewhere, i.e. the capacitance given by the elementary approximation mentioned in § 1.

Capacitance is given by an integral of charge density σ over the area of either plate:

$$C = \frac{1}{V}\int \sigma \, dA. \tag{22}$$

Since the charge density on a conducting surface is proportional to the field strength perpendicular to it, for the geometry of figure 4(*a*) the capacitance per unit length in the direction parallel to the edge of the upper electrode is given by

$$\frac{\partial C}{\partial l} = \frac{\varepsilon}{V}\int E_y \, dx \tag{23}$$

where ε is the dielectric constant of the medium.

Consider first the fringing capacitance due to excess charge on the lower side of the upper electrode. This is given by

$$\frac{\partial C_L}{\partial l} = \frac{\varepsilon}{V} \int_C^B \left(E_y - \frac{V}{\pi a} \right) dx. \tag{24}$$

If we put $w = -p$ with p real and positive, we obtain, from equation (10),

$$dx = \left(\frac{a-p}{p} \right) dp \tag{25}$$

and, from equation (14),

$$E_y = \frac{V}{\pi(a-p)}. \tag{26}$$

Substitution in equation (24) yields

$$\frac{\partial C_L}{\partial l} = \frac{\varepsilon}{\pi}. \tag{27}$$

Interestingly, this result is independent of any dimension of the electrode geometry other than the length of the perimeter. The numerical value of equation (27) in vacuum or air is 2.82 pF m^{-1}.

We turn now to the second component of fringing capacitance for the geometry of figure 4(a), that due to charge on the upper surface of the bounded electrode. This may be written

$$\frac{\partial C_U}{\partial l} = \frac{\varepsilon}{V} \int_B^A (E_y - 0)\, dx \tag{28}$$

and, repeating the above substitutions, we obtain

$$\frac{\partial C_U}{\partial l} = \frac{\varepsilon}{\pi} \lim_{p \to \infty} \ln \frac{p}{a} \tag{29}$$

which is unbounded. Clearly this cannot represent the fringing capacitance of any electrode of finite dimensions. The integral diverges at the point A because, as may be readily shown, E_y varies as x^{-1} as $x \to -\infty$. For any electrode of finite extent, the upper fringing capacitance will be more correctly, though only approximately, represented by

$$\frac{\partial C_U}{\partial l} \approx \frac{\varepsilon}{\pi} \ln \pi P/d \tag{30}$$

where P is a dimension characteristic of the width of the electrode, for example the diameter of a disc. The total fringing capacitance, C_f, is then given by

$$C_f \approx \frac{\varepsilon L}{\pi} \ln \frac{\pi e P}{d} \tag{31}$$

where L is the length of perimeter of the bounded electrode. For $P/d = 10$ the fringing capacitance is 12.5 pF per metre of perimeter, and increases by 6.5 pF m^{-1} for each decade increase in P/d. Uncertainty in defining and estimating the parameter P imposes a limitation on the utility of equation (31), particularly for electrodes of irregular shape. A factor of two error in P, for example, will introduce an error of 2.0 pF m^{-1} in C_f.

For a disc capacitor of radius R equation (31) leads to a simple first-order approximation to the actual capacitance C:

$$C \approx C_{\text{elem}}\left(1+\frac{2d}{\pi R}\ln\frac{2e\pi R}{d}\right) \tag{32}$$

where $C_{\text{elem}} = \pi\varepsilon R^2/d$ is the elementary capacitance calculated from the uniform field model. The literature contains several such first-order estimates of C, derived in various ways, but quite similar in form. A convenient summary is given by Sneddon (1966). In the notation of this paper, they include the expression due to Kirchhoff (1877) and more rigorously derived by Hutson (1963):

$$C \approx C_{\text{elem}}\left(1+\frac{2d}{\pi R}\ln\frac{8\pi R}{ed}\right) \tag{33}$$

a modification of equation (33) proposed by Ignatowsky (1932):

$$C \approx C_{\text{elem}}\left(1+\frac{2d}{\pi R}\ln\frac{32R}{ed}\right) \tag{34}$$

and an approximation given by Cooke (1958) based on an idea of Maxwell (1866):

$$C \approx C_{\text{elem}}\left(1+\frac{2d}{\pi R}\ln\frac{\pi eR}{d}\right). \tag{35}$$

The notation in these expressions is consistent with that used throughout this paper in that d denotes the distance between a disc and a plane. The expressions may be applied to two-disc electrode systems by taking the electrode separation as $2d$.

The values given by equations (32)–(35) may be compared with precise numerical data given by Cooke (1958) and Bartlett and Corle (1985); the results are plotted in figure 5†. It will be seen that, of the first-order approximations, equation (32) generally gives the best results, although not necessarily for larger R/d. All four estimates are asymptotically correct for large R/d since $C/C_{\text{elem}} \to 1$ as $R/d \to \infty$.

None of the first-order estimates is satisfactory for R/d less than about 4 and approximations differing in form from equations (32)–(35) are required in this case. Leppington and Levine (1970) and Shaw (1970) have given approximations which improve on the Kirchhoff–Hutson expression by the inclusion of higher-order terms, while Sneddon (1966) has given a closed-form expression whose accuracy is good for small, but not large, R/d. Empirically we have found that the expression

$$\frac{C}{C_{\text{elem}}} \approx 1+\frac{2d}{\pi R}\ln\frac{8\pi R}{ed}+\left(\frac{d}{\pi R}\ln\frac{d}{8\pi R}\right)^2 \tag{36}$$

gives good accuracy down to quite small disc radii. Equation (36) is obtained by deleting from the full second-order approximation of Shaw (1970) a term in $(d/R)^2$ whose coefficient, labelled $C^{(3)}$ by Shaw, involves a definite integral‡. The error of equation (36) is plotted in figure 5, where its superiority to any of the first-order approximations is readily apparent.

† It should be noted that the values tabulated by Cooke (1958) and quoted by Sneddon (1966) for the Maxwell–Cooke method are not derived from equation (35). They are calculated from a more exact equation of transcendental type, not in closed form, which approximates to equation (35) for large R/d. Also the values given by Sneddon for the Kirchhoff–Hutson method appear to be erroneous and considerably underestimate the error of equation (33).

‡ We suspect, on the basis of an unsuccessful attempt at numerical evaluation, that this integral may not exist.

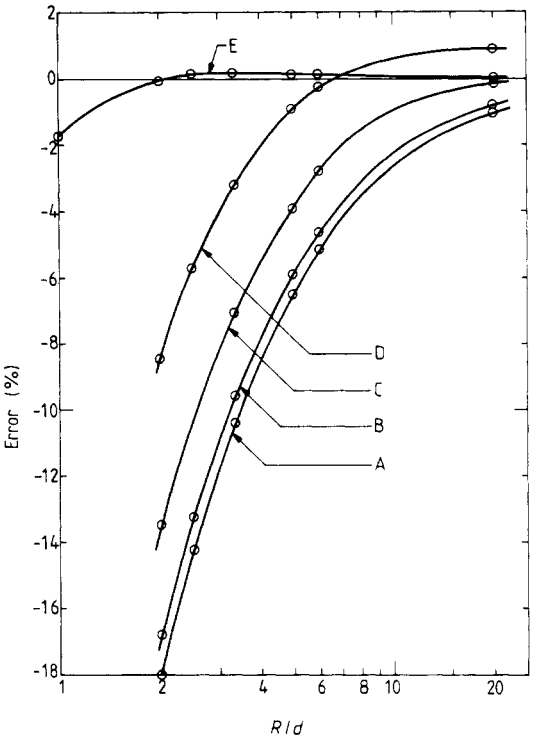

Figure 5. Errors in estimates of the capacitance of disc capacitors compared with numerical data of Bartlett and Corle (1985) for $R/d = 6$ and Cooke (1958) for all other points: A, Maxwell-Cooke; B, Kirchhoff-Hutson; C, Ignatowsky; D, equation (32); E, equation (36). Here d denotes the electrode separation for a disc and plane system, or half the electrode separation for a two-disc system.

Acknowledgment

We wish to thank G W Small for helpful comments on theoretical aspects of this work.

References

Atkinson W J, Young J H and Brezovich I A 1983 *J. Phys. A: Math. Gen.* **16** 2837
Bartlett D F and Corle T R 1985 *J. Phys. A: Math. Gen.* **18** 1337
Carrier G F, Krook M and Pearson C E 1966 *Functions of a Complex Variable* (New York: McGraw-Hill) pp 315-6
Cooke J C 1958 *Z. Agnew. Math. Mech.* **38** 349
DiStasio M and McHarris W C 1979 *Am. J. Phys.* **47** 440
Harrison J A 1967 *Br. J. Appl. Phys.* **18** 1617
Hughes B D 1984 *J. Phys. A: Math. Gen.* **17** 1385
Hutson V 1963 *Proc. Camb. Phil. Soc.* **59** 211
Ignatowsky W 1932 *Acad. Sci. URSS Trav. Inst. Stekloff* **3** (2) 1
Kirchhoff G 1877 *Monatsb. Acad. Wiss. Berlin* 144-62
Kober H 1957 *Dictionary of Conformal Representation* (New York: Dover)
Leppington F and Levine H 1970 *Proc. Camb. Phil. Soc.* **68** 235
Love E R 1949 *Quart. J. Mech. Appl. Math.* **2** 428
Maxwell J C 1866 *Phil. Trans. R. Soc.* **156** 249

—— 1904 *A Treatise on Electricity and Magnetism* (Oxford: Clarendon) 3rd edn, ch XII

Nicholson J W 1924 *Phil. Trans.* A **224** 303

Shaw S J N 1970 *Phys. Fluids* **13** 1935

Sloggett G J, Clothier W K, Benjamin D J, Currey M F and Bairnsfather H 1984 *Precision Measurement and Fundamental Constants II. NBS Spec. Publ. 617* ed B N Taylor and W D Phillips (Washington, DC: NBS) p 469

Sneddon I N 1966 *Mixed Boundary Value Problems in Potential Theory* (Amsterdam: North-Holland) p 230